

Contribution of Soil, Sulfate, and Biomass Burning Sources to the Elemental Composition of PM₁₀ from Mexico City

Barrera, V.A.¹, Miranda, J.^{1*}, Espinosa, A.A.¹, Meinguer, J.¹, Martínez, J.N.¹, Cerón, E.¹,
Morales, J.R.², Miranda, P.A.² and Dias, J.F.³

¹Instituto de Física, Universidad Nacional Autónoma de México, A.P. 20-364, México, D.F., Mexico

²Departamento de Física, Facultad de Ciencias, Universidad de Chile, Las Palmeras 3425, Ñuñoa, Santiago, Chile

³Universidade Federal do Rio Grande do Sul, Porto Alegre, Brazil

Received 22 July 2011;

Revised 10 Jan. 2012;

Accepted 22 Jan. 2012

ABSTRACT: This study is aimed to identify sources of particulate matter with mean aerodynamic diameter below 10 μm (PM₁₀) present in the atmosphere of the Metropolitan Area of Mexico City (MAMC), using samples obtained from January 1st to June 30th, 2009, analyzed with X-ray spectrometric techniques. MiniVol samplers were used to collect samples on polycarbonate filters in three sites (North, Center, and South) of the MAMC. The filters were exposed along 24 h every two days, starting at 8:00 AM, and then analyzed with particle induced X-ray emission (PIXE), a microPIXE (μPIXE) system, and X-ray fluorescence (XRF). Statistical multivariate tests with positive matrix factorization (PMF) were conducted to identify possible contributing factors. The model HYSPLIT was used to determine back-trajectories and the MODIS database for fire spot localization. The multivariate methods identified five factors in the Center and South, and four in the North, including Soil, Sulfate, Fuel/Industry, and Biomass burning, with certain differences in the factors and contributions. Application of HYSPLIT back-trajectories associated these factors to three main Soil sources and points of secondary aerosols production, as well as locations where Biomass burning aerosols were originated. The combination of X-ray spectrometric methods, receptor modeling, back-trajectory determination, and fire site localization, allowed the identification of possible sources of PM₁₀ in the MAMC, namely, the dry Texcoco lake, the Toluca Valley, and the North dry plains for Soil aerosols, the influence of local industrial areas for Sulfate (secondary) aerosols, and the appearance of fires for Biomass burning.

Key words: Aerosols, Mexico City, PIXE, μPIXE , XRF, PMF

INTRODUCTION

Different elements influencing the air quality have been regarded within different studies (Montero Lorenzo *et al.*, 2011; Zou *et al.*, 2011; Nejadkoorki and Baroutian, 2012). The first studies on the elemental composition of total airborne suspended particulate matter (TSP) in the Mexico City Metropolitan Area (MCMA) were carried out by Navarrete *et al.* (1974), Barfoot *et al.* (1984) and Aldape *et al.* (1991a, 1991b). In the last two decades, more than 50 papers were published using different methods to analyze their composition. Currently, a systematic monitoring program on aerosols with Mean Aerodynamic Diameters (MAD) below 10 μm (PM₁₀)

and 2.5 μm (PM_{2.5}), is being conducted by the Atmospheric Monitoring Automatic Network (RAMA) in MAMC. Although this program is limited to the measurement of gravimetric mass concentrations using an oscillating microbalance type samplers (TEOM[®], Rupprecht & Patashnick, East Greenbush, NY, USA), it has helped to improve the air quality in MCMA. Undoubtedly, the most comprehensive study of air pollution in MCMA took place in 2006 through the MILAGRO campaign (Molina *et al.*, 2010). Nevertheless, the sources of particulate matter related to soils or fugitive dust are still not fully identified. In this regard, before the MILAGRO project, Vega *et al.*

*Corresponding author E-mail: miranda@fisica.unam.mx

(2002) explained that “Geological material was the major component of PM_{10} , accounting for 37.4%” of the total mass, and its origin was assigned to agricultural lands around MCMA in the north and northeast sectors of the basin. In turn, Johnson *et al.* (2006) observed an increase in fine soil concentration being associated to particle back-trajectories passing up the Rio Balsas valley and over Toluca to the west/southwest of the Mexico City basin (de Foy *et al.*, 2006). Along with the low Na and Cl concentrations (around $0.1 \mu\text{g}/\text{m}^3$), these results disfavor dry Texcoco lake as the dominant source of soil particles, as it was suggested by other authors (Moya *et al.*, 2003). In this work, the authors emphasize that the most important contribution to inhalable aerosols comes from the coarse fraction PM_{10} . The origin of soil-derived aerosols was not explicitly mentioned by Molina *et al.* (2010) in their MILAGRO summary, although they cite the works done on the elemental analysis during the campaign. Querol *et al.* (2008) determined that in Southwest Mexico City samples, soil-derived aerosols probably represent mineral dust resuspension in the city, without any specific identification of the emitting sources. More recently, application of chemical mass balance (CMB) model (Vega *et al.*, 2009) showed significant spatial variations in source contributions, which are influenced by local (not specified) soil types and land use. In summary, different studies do not fully agree in the identification of the origin of soil-derived particles in the atmosphere of MCMA. This work is aimed to study the contribution of some potential soil dust sources using elemental analysis of PM_{10} samples collected in three representative sites of MCMA. Statistical techniques such as absolute principal component analysis (APCA) and positive matrix factorization (PMF), together with the reconstruction of back-trajectories through the open access model HYSPLIT (Draxler and Rolph, 2010; Rolph, 2010) were used in this study. In the past, examples of the combination of PIXE and XRF, PMF, and back-trajectories have been developed successfully (Cohen *et al.*, 2010; Chiou *et al.*, 2009) to determine source contributions.

MATERIALS & METHODS

Aerosol samples were deposited onto 47 mm diameter, $0.4 \mu\text{m}$ pore size polycarbonate filters (Nuclepore, Costar Corp.) using MiniVol portable samplers, every two days, for 24 h periods starting at 8:00 AM, from January 1st to June 30th, 2009. Samplers were located at roof top level (between 2.5 m and 12 m). The sampling sites (Fig. 1) were placed in the North (*Instituto Mexicano del Petróleo*, IMP), Center (the *Palacio de Minería* building), and South (*Instituto de Física*, main UNAM campus). Samples were analyzed with PIXE, using a 2.2 MeV proton beam produced by

the 3.75 MV Van de Graaff Accelerator at Universidad de Chile, Chile. The protocols for PIXE application, including the measurement of the detection system efficiency with an RM 8785 National Institute of Standards and Technology (Gaithersburgh, MD, USA) urban particulate matter standard, are better described elsewhere (Miranda *et al.*, 2006). In the case of XRF, an analyzing system was constructed, based on an Rh anode X-ray tube and an Amptek Si-PIN detector. The calibration of this device was carried out by means of MicroMatter thin film standards. A voltage of 50 kV and anode current of $750 \mu\text{A}$ was set, irradiating each filter during 900 s; the primary X-ray beam had a 5 mm diameter. Also, gravimetric mass was determined using a 210D Ohaus electrobalance (resolution $10 \mu\text{g}$). Temperature during gravimetric mass measurements oscillated between $20 \text{ }^\circ\text{C}$ and $25 \text{ }^\circ\text{C}$, while relative humidity was in the range 30% - 40%; filters were pre-conditioned during 24 h within similar temperature and relative humidity ranges. PIXE results allowed the identification of episodes possibly related to soil particles or biomass burning, so those specific filters were studied with μPIXE employing the Oxford Microprobe (Oxford, UK) nuclear microprobe installed at the Universidade Federal do Rio Grande do Sul, Brasil. A beam of 3 MeV protons was focused to a spot of diameter within $2 \mu\text{m}$ to $3 \mu\text{m}$ to irradiate an area of $100 \times 100 \mu\text{m}^2$ in order to obtain elemental mappings at three locations in each selected sample. It must be mentioned that there was not an important superposition of particles on the filters, because of the use of MiniVol (low volume) samplers, a fact tested with optical microscopy observations; furthermore, no quantitative analyses were attempted, so the possible effect of particle accumulation is even lower. Thus, the μPIXE results effectively come from single particles only. The computer code GUPIX (Maxwell *et al.*, 1995) was used to analyze PIXE spectra while QXAS (IAEA, 1997) was applied to XRF spectra.

Once the elemental concentrations were determined, the multivariate statistical analysis technique Positive Matrix Factorization (PMF) (Paatero and Tapper, 1994) method was used to look for an alternative identification of emitting sources. The evaluation of the experimental uncertainties in elemental concentrations, required in PMF applications, was done following the procedure explained by Espinosa *et al.* (2010).

Concerning the meteorological parameters, they were obtained from stations belonging to the *Programa de Estaciones Meteorológicas del Bachillerato Universitario*, managed by the *Centro de Ciencias de la Atmósfera*, UNAM, located near to the sampling sites (not farther than 1 km). Also, the databases



Fig. 1. Location of the sampling sites

obtained by the Automatic Monitoring System (SIMAT) in the MAMC were used for SO₂ concentrations data.

RESULTS & DISCUSSION

PIXE analyses allowed the identification of 14 elements (Al, Si, S, Cl, K, Ca, Ti, V, Cr, Mn, Fe, Ni, Cu, and Zn), although not all of them were found in each sample (Cr in less than 50% of the samples). Moreover, XRF gave information on Se and Pb contents, being detected in less than 50% of the samples. A total of 146 valid samples could be used in the analysis: 50 from the North, 45 from the Center, and 51 from the South; the sampling periods were the same for all three sites. Mean gravimetric mass and elemental concentrations are summarized in Table 1. The South site is located in a mostly residential area with medium traffic load, while the North site is in an industrial district, with heavy traffic. The Center site presents usually heavy traffic most of the time. As it has been reported previously (Miranda *et al.*, 1998; Miranda *et al.*, 2004; Miranda *et al.*, 2005), the South site presents lower mass and elemental concentrations, as compared to the other two sites. Moreover, Table 1 displays a comparison among the results for PM₁₀ elemental concentrations determined at the Center site during 2002 (Miranda *et al.*, 2005), and in 2009. It is interesting to find very similar values for the most important elements in both studies.

It is important to mention that the sampling period was influenced by two relevant facts: firstly, due to the AH1N1 epidemics, all activities in the MCMA were suspended and, secondly, the first half of the year 2009 suffered from a remarkably dry weather. Because of the suspension of urban activities it was not possible to collect samples from April 25 to May 6 in the North and Center sites. Fig. 2 shows a comparison of the total elemental mass measured with PIXE and the wet precipitation in the South site for the whole period. It is observed that in the period when the activities were suspended there was not a significant decrease in the total elemental mass concentrations determined by PIXE. There was an episode during May 4 to May 7, during the activities suspension. This fact strongly suggests that the main contributor to the measured mass is not from anthropogenic origin. Fig. 3 presents a wind rose for the Center site, showing that the winds came from the east and south, which coincide with what will be shown below using back-trajectories. This is in partial agreement with the proposed sources of soil-derived particles that had been mentioned in previous works (Moya *et al.*, 2003), although no sources in the south have been described before. In addition, contribution from re-suspended dust due to vehicular traffic is not expected in the suspension period. This is in contrast with the assertion that probably dust re-suspension explains the geological material found in PM₁₀ (Querol *et al.*, 2008), but a single

Table 1. PM_{10} mean elemental concentrations in 24 h (in $\mu\text{g}/\text{m}^3$)

Element	North	Center	South	Center 2002 (Miranda et al. 2005)
Valid samples	50	45	51	-
Mass	71.1 (3.8) ^a	80.8 (6.9)	66.7 (4.4)	-
Al	0.89 (0.76)	0.63 (0.31)	0.49 (0.27)	1.25 (0.14)
Si	4.4(3.4)	3.1 (1.5)	2.5 (1.4)	3.2 (0.35)
S	1.4 (1.1)	1.3 (0.59)	0.92 (0.46)	1.40 (0.11)
Cl	0.20 (0.19)	0.20 (0.39)	0.094 (0.095)	0.29 (0.06)
K	0.73 (0.64)	0.45 (0.25)	0.43 (0.29)	0.51 (0.05)
Ca	2.5 (2.1)	1.3 (0.52)	1.04 (0.62)	1.7 (0.14)
Ti	0.096 (0.071)	0.071 (0.034)	0.068 (0.039)	0.090 (0.008)
V	0.048 (0.089)	0.017 (0.028)	0.016 (0.029)	0.019 (0.004)
Cr ^b	0.019 (0.038)	0.003 (0.005)	0.005 (0.010)	0.012 (0.002)
Mn	0.066 (0.091)	0.013 (0.009)	0.018 (0.018)	0.055 (0.011)
Fe	1.20 (0.88)	0.84 (0.34)	0.76 (0.39)	0.84 (0.097)
Ni	0.011 (0.013)	0.012 (0.020)	0.006 (0.008)	0.006 (0.001)
Cu	0.036 (0.033)	0.045 (0.029)	0.031 (0.024)	0.020 (0.002)
Zn	0.19 (0.16)	0.095 (0.047)	0.064 (0.037)	0.088 (0.010)
Se ^b	0.37 (0.25)	0.063 (0.30)	-	-
Pb ^b	0.095 (0.077)	0.088 (0.058)	0.077 (0.063)	0.024 (0.003)

^a Numbers between parenthesis represent the standard deviation

^b This element was present in less than 50% of the samples

event may not be enough to discard this suggestion. In a different aspect, there is a small growth in the rainfall after May 14, with an expected decrease in the measured particle mass, as noted in Fig. 2, also.

Now, it is possible to follow with the development of the receptor models using PMF. The number of samples is above the minimum necessary to apply this method (Hopke, 1991), although it would have been desirable to obtain more samples. It is fundamental to mention that in this work the models are referred to the total gravimetric mass. As an average, total PIXE plus XRF mass represents 13% of gravimetric mass in the Center site, 18% in the North site, and 14% in the South site. The ratio of PIXE plus XRF mass to gravimetric

mass is shown in Fig. 4, where it is seen that the sum of elemental measured mass was higher for the cold-dry season (January to March). The unexplained mass must undoubtedly come from organic carbon (OC), elemental carbon (EC), oxygen, nitrates, or other compounds/elements not detected by PIXE or XRF. To obtain absolute source contributions, in PMF the total gravimetric mass was included in the computing with the *EPA-PMF* computer code (EPA, 2010). Using this program, it was possible to repeat the calculation until the most appropriate number of factors was reached, looking at the Q value (10900 for Center, 10200 for North, and 9500 for South), and the F and G matrices. Additionally, different F_{PEAK} values were

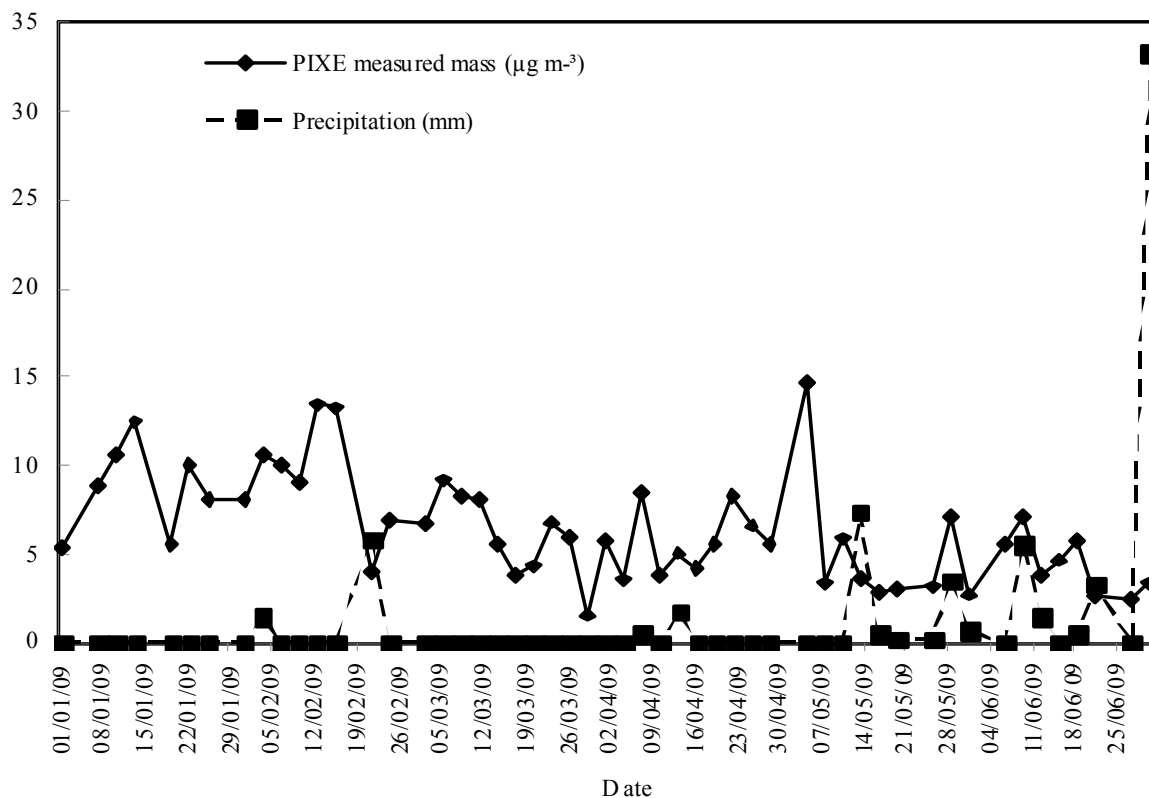


Fig. 2. Time series of total mass measured with PIXE and precipitation in the South site

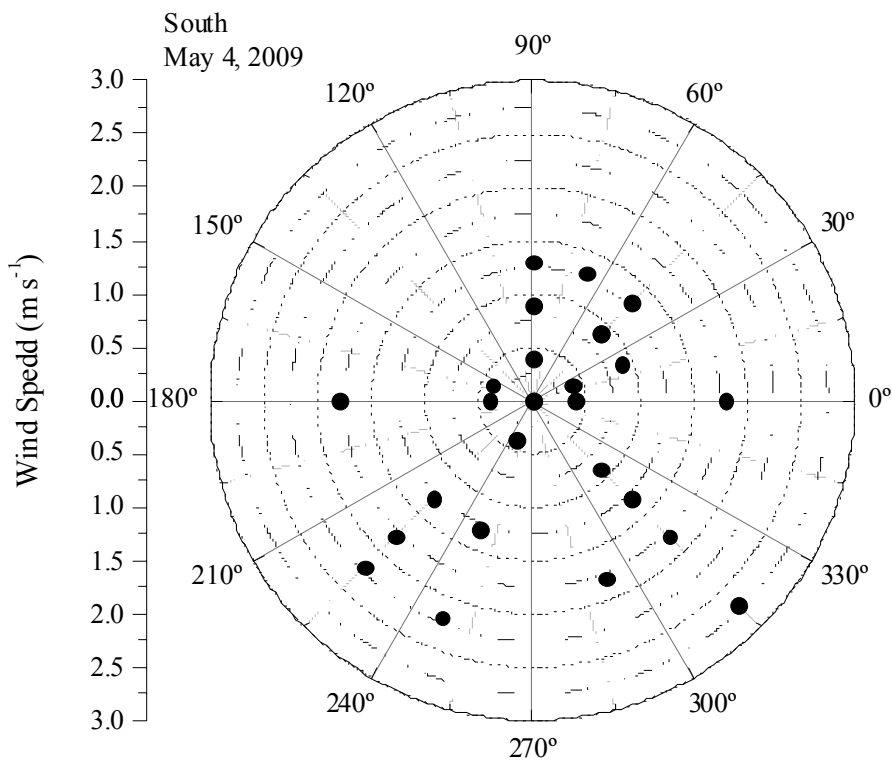


Fig. 3. Wind rose for the South site on May 4, 2009. The dots represent data for wind direction and speed. The East direction is located as 0°

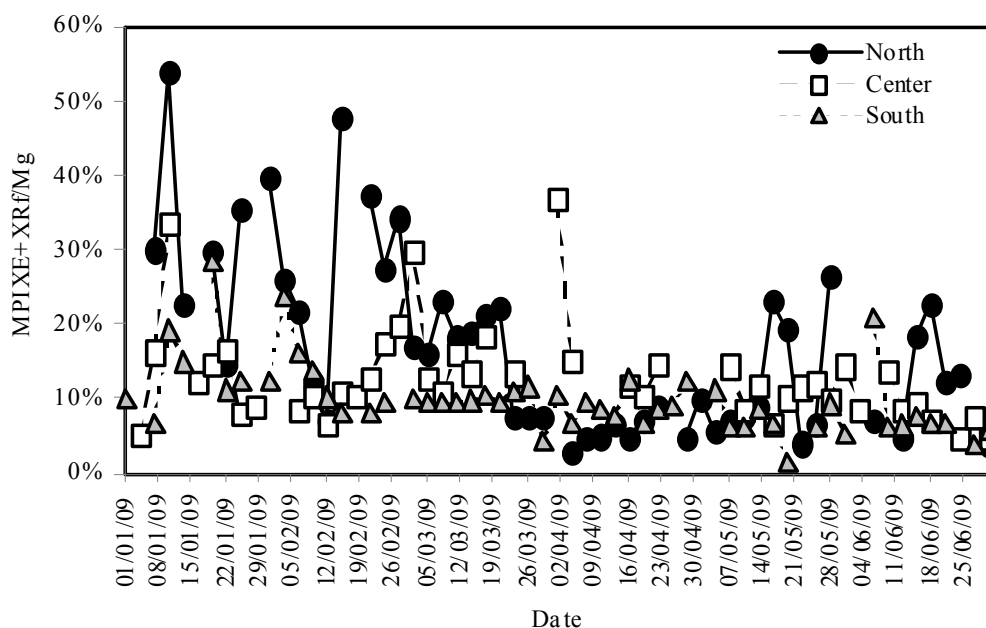


Fig. 4. Ratio of total PIXE + XRF mass to gravimetric mass (M_g) for the three sampling sites

tested; for North and South $F_{PEAK} = 0.1$ gave the best results, while $F_{PEAK} = 0.2$ was more appropriate for Center. All of the runs converged, while most residuals for all detected elements were low, except for some episodes. Increasing the number of sources only resulted in the appearance of factors with a null contribution to total gravimetric mass; therefore, the number reported here is considered as the most appropriate. Table 2 summarizes all the factors determined with both methods, with the elements included in each factor and the fraction contributed by each factor to the total gravimetric mass. The elements Cr, Se and Pb were not considered because, as mentioned earlier, they were found in less than 50 % of the samples; V and Ni had very small contributions, because of their low concentrations. It is possible to see that PMF identifies two types of “soil” sources for Center and South. There are other important contributors to PM_{10} , like biomass burning, with elements in full agreement with those reported by the database *Speciate* (Speciate, 2009); sources labeled as “agricultural vegetative burning”, “vegetative burning” or “wildfires” contain all the elements found in those factors with PMF with similar profiles as those determined in this work. Also, there are secondary aerosols (labeled in this work as “sulfate”), which are characterized by the correlation of S with “soil” elements; this fact was already observed before in the MAMC (Miranda *et al.*, 2005). A final factor is related to “industry/fuel oil” emission sources. This factor might also be related to traffic/vehicle emissions, but the presence of the S-V-Ni group usually marks to fuel oil combustion (Miranda *et al.*, 2004). To check the

accuracy of the predictions made by PMF, the mass predicted by the multivariate method is plotted in Fig. 5 as a function of the gravimetric mass, for the Center site; the agreement for both methods is excellent, with similar findings for the North and South sites. As expected, the largest fraction comes from the “soil” components. Time series of the contributions from “soil” factors in the three sites for PMF are shown in Fig. 6. It is apparent that there are several episodes along the sampling period.

It was also noticeable that S is often found as a component in “soil” factors (see, in particular, the North results in Table 2), and also the identification of “sulfate” sources, which actually contain elements with a geological origin (Al, Si, Ca, Fe), too. Additionally, the sources identified as “biomass burning” showed a few episodes. Therefore, it was necessary to check if particles with those assigned factors are real or if it was only an artifact of the statistical model. Samples that showed a high concentration of the aforementioned possible sources were then analyzed with μ PIXE. Due to the large number of available samples, only 15 among those filters, which were associated with episodes in the factors described by the receptor models, were analyzed with μ PIXE, choosing three spots per sample. Two examples of the results are displayed in Figs. 9 and 10 (Center, January 19; South, February 15, respectively). Aside from the particles including the common “soil” elements Si, K, Ca, Ti, Mn, and Fe, many particles with these elements also contain S, corroborating the results obtained with PMF. An association of the ion SO_4^{2-} and the elements

Table 2. Factors determined in PM₁₀ with the application of PMF showing associated elements and contribution of each factor to total gravimetric mass

Factor	North	Center	South
1	Sulfate	Industry/Fuel	Industry/Fuel
	Al, Si, S, K, Ca, Ti, Fe	S, Ca, V, Fe, Ni, Cu, Zn	Si, S, K, V, Ni, Cu, Zn
	2.6%	2.5%	1.4%
2	Soil	Sulfate	Soil 1
	Al, Si, K, Ca, Ti, Mn, Fe	Al, Si, S, K, Ca, Ti, Fe	Si, S, K, Ca, Fe
	8.7%	4.3%	5.4%
3	Biomass burning	Biomass burning	Sulfate
	Si, S, Cl, K, Ca	Al, Cl, K, Ca, Fe	Al, Si, S, K, Ca, Fe
	3.4%	0.8%	3.2%
4	Industry/Fuel	Soil 1	Soil 2
	S, V, Fe, Ni, Cu, Zn	Al, Si, K, Ca, Ti, Mn, Fe	Al, Si, K, Ca, Ti, Fe
	4.3%	3.7%	2.6%
5	-	Soil 2	Biomass burning
		Al, Si, K, Ca, Ti, Fe, Zn	Si, S, Cl, K
		2.1%	1.3%

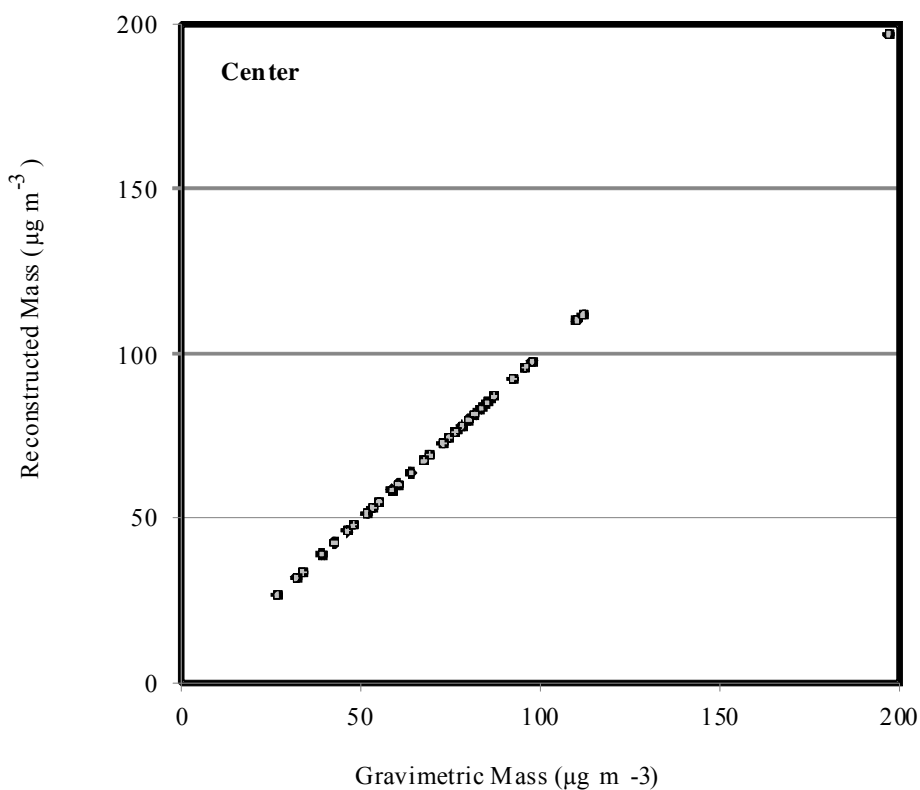


Fig. 5. Comparison of the total mass measured with PIXE and the prediction by PMF, for the Center site

Elemental Composition of PM_{10}

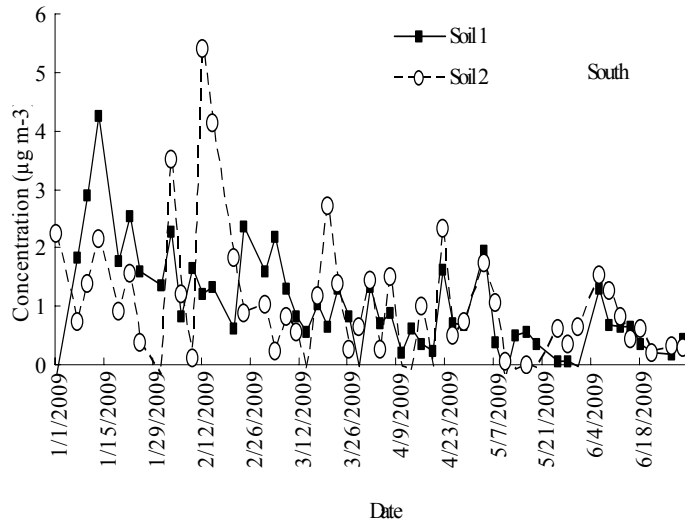
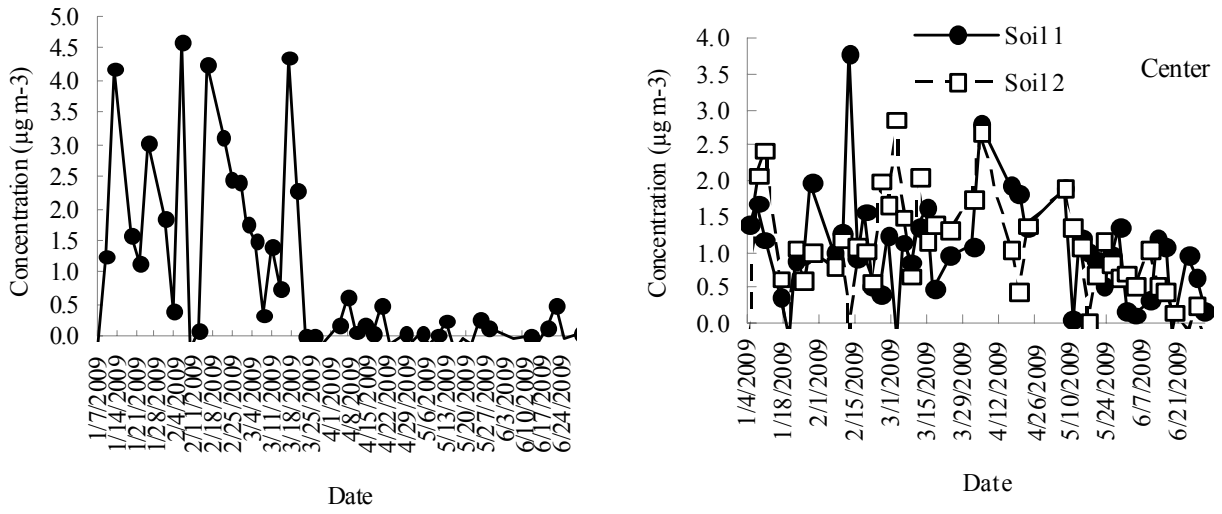


Fig. 6. Time series of the contributions from “soil” factors in the three sites for PMF

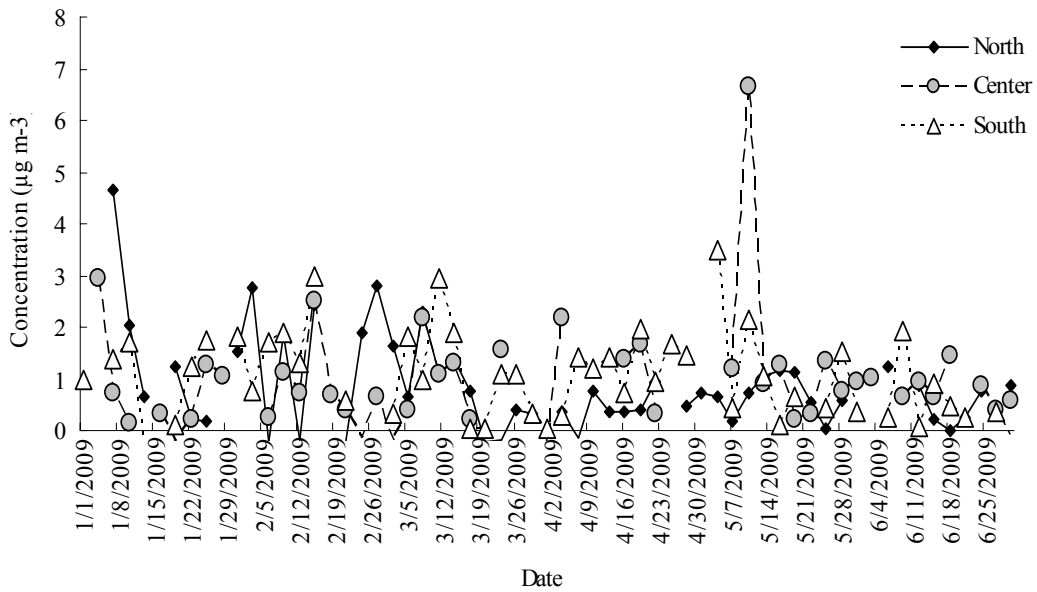


Fig. 7. Time series of the contributions from “sulfate” factors in the three sites for PMF

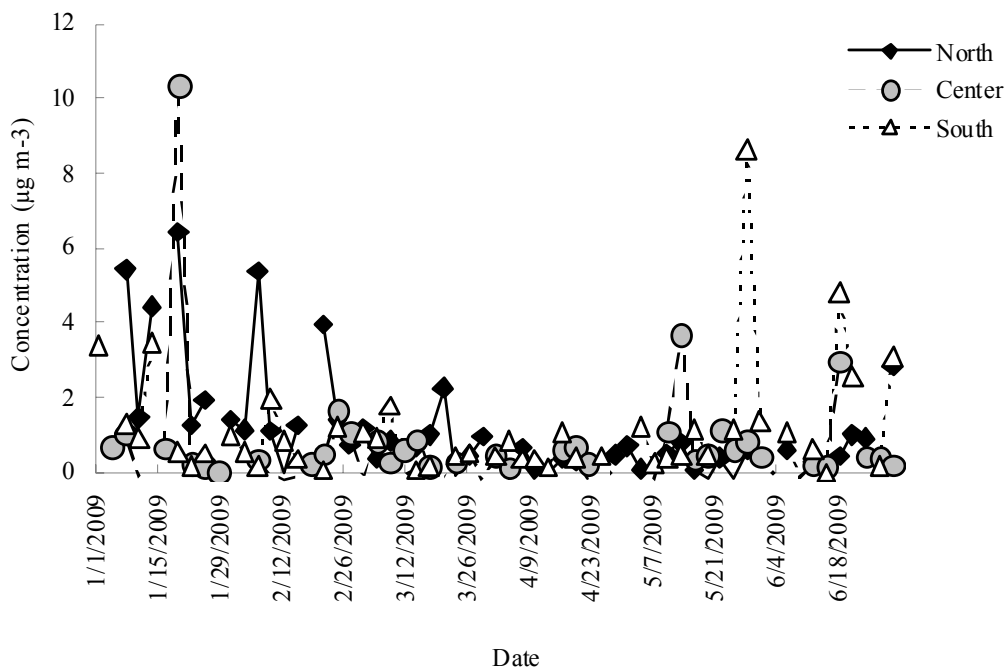


Fig. 8. Time series of the contributions from “biomass burning” factors in the three sites for PMF

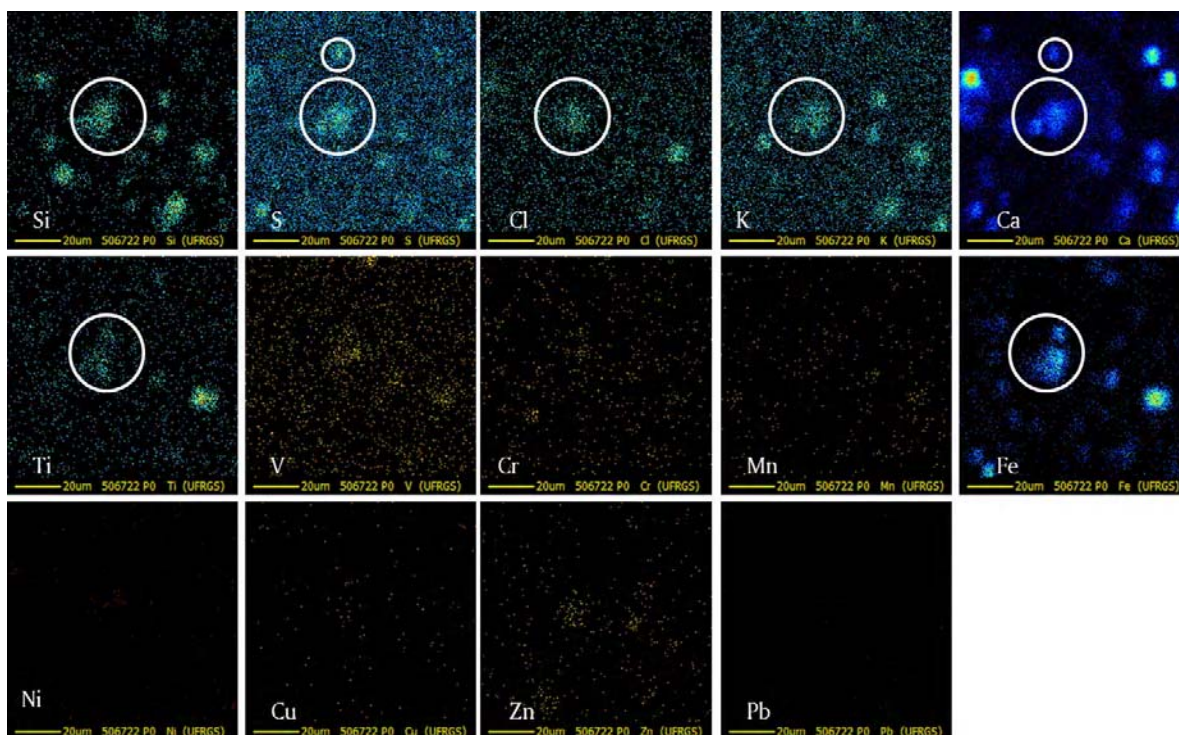


Fig. 9. µPIXE elemental mappings for the sample collected on the Center site, January 19, 2009. The large circles correspond to a particle containing Si, S, K, Ca, Ti, and Fe, while the small circles identify a particle containing S and Ca

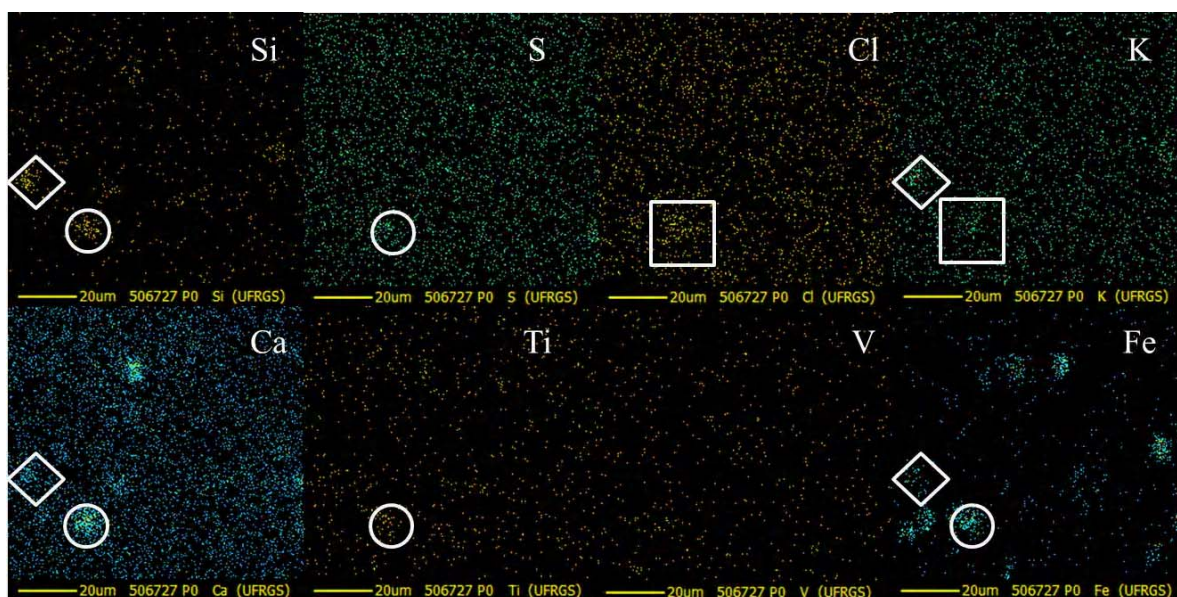


Fig. 10. μ PIXE elemental mappings for the sample collected on the South site, February 15, 2009. The circles correspond to a particle containing Si, S, Ca, Ti, and Fe; the squares to a particle with Cl and K; the diamonds to a particle containing Si, K, Ca, and Fe

K and Ca has been observed earlier in the South site (Báez *et al.*, 2007), supporting the present results. As mentioned above, most probably these are not particles coming from an S-rich type of soil, but rather fugitive dust particulate matter subjected to atmospheric S chemical reactions (secondary aerosols). This kind of processes has already been observed by other authors (Jeong and Park, 2008). In this regard, it is very difficult to associate with confidence any specific emitting source to the resulting factors.

As a first attempt to determine the definite source of the particles with a geological origin, the profiles of the “soil” factors found with PMF are compared with the results obtained in the extensive work published by Vega *et al.* (2001). It may be done, as above, through the calculation of elemental concentration ratios relative to Si for each kind of fugitive dust emitter studied by Vega and coworkers (2001). The results are shown in Fig. 11, considering PM_{10} elemental composition. Although in earlier papers an association with the dry Texcoco Lake was found (Miranda *et al.*, 2004; Miranda *et al.*, 2005), in the present work there are no definite similarities for the PMF “soil” factors, with an important presence of S in Soil 2/Center, Soil/North, and Soil 2/South. Nonetheless, PMF Soil 1/Center and Soil 1/South have a certain similarity with Dry Lake, having a visible enrichment with Fe, which is also appreciated in every “soil” factor. In contrast, it is convenient to say that the profile of the PMF Soil 2 factor in the South presents very similar concentration ratios to those calculated in a previous study in the same site for the year 1996 (Miranda *et al.*, 2000). The concentration ratios for K are 0.052

and 0.050 for PMF in 2009 and APCA in 1996, respectively; for Ca both are equal to 0.319; for Ti, 0.016 and 0.033; for Fe, 0.241 and 0.213. The difference comes from the presence of S in the present study for Soil 2/South. It seems that the Soil 2 source is actually a “soil” emission subjected to chemical reactions with S compounds. It is inferred, then, that the only fugitive dust source analyzed by Vega *et al.* (2001) that may be in fair agreement with the present study is the Dry Lake, with some chemical influence from other sources (adding elements like S, Ca, and Fe).

In order to have a more definite recognition of the origin of soil-derived particulate matter, the simulation model Hybrid Single-Particle Lagrangian Integrated Trajectory, better known as HYSPLIT (Draxler and Rolph, 2010; Rolph, 2010), was employed to calculate back-trajectories during the episodes identified in each site using PMF. A period of 24 h (24 trajectories per day, with a point every hour), and two different heights (500 m and 1000 m, as recommended) above ground level were taken into account for the simulations, to overcome the low resolution limitations of the simulation software. Due to the spatial resolution of HYSPLIT, it was not possible to obtain different backtrajectories for each sampling site; the same was found for the three sites. The time period was chosen to coincide with beginning and the end of the sample collection time, and to look for proximate possible sources, but not necessarily from long-range transport. It was noticed that, in the majority of cases, the sets of back-trajectories did not have a wide spread, making it feasible to identify the possible provenance of the

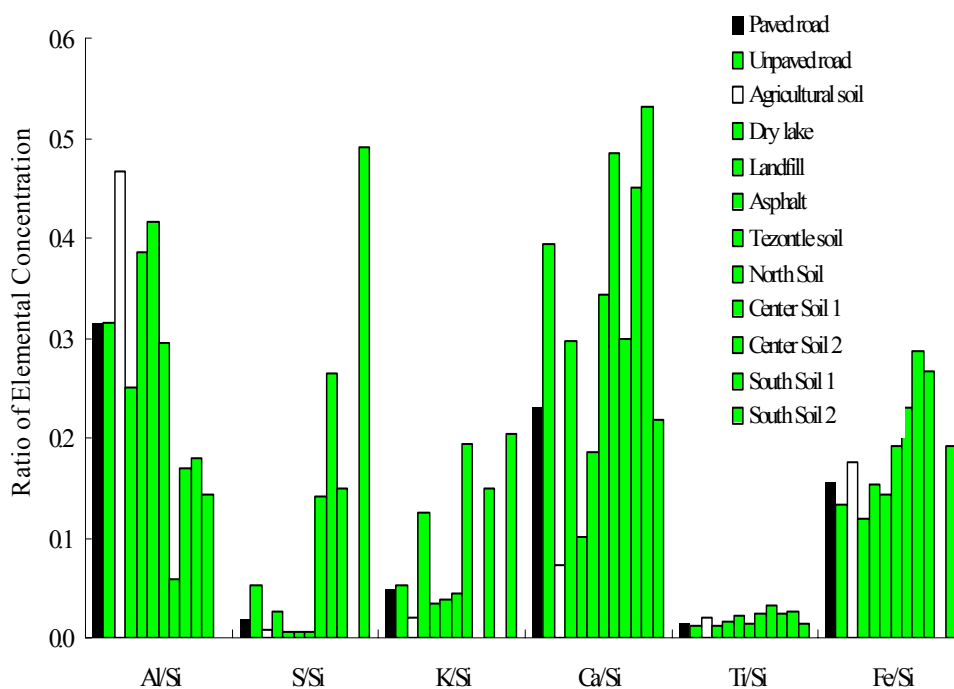
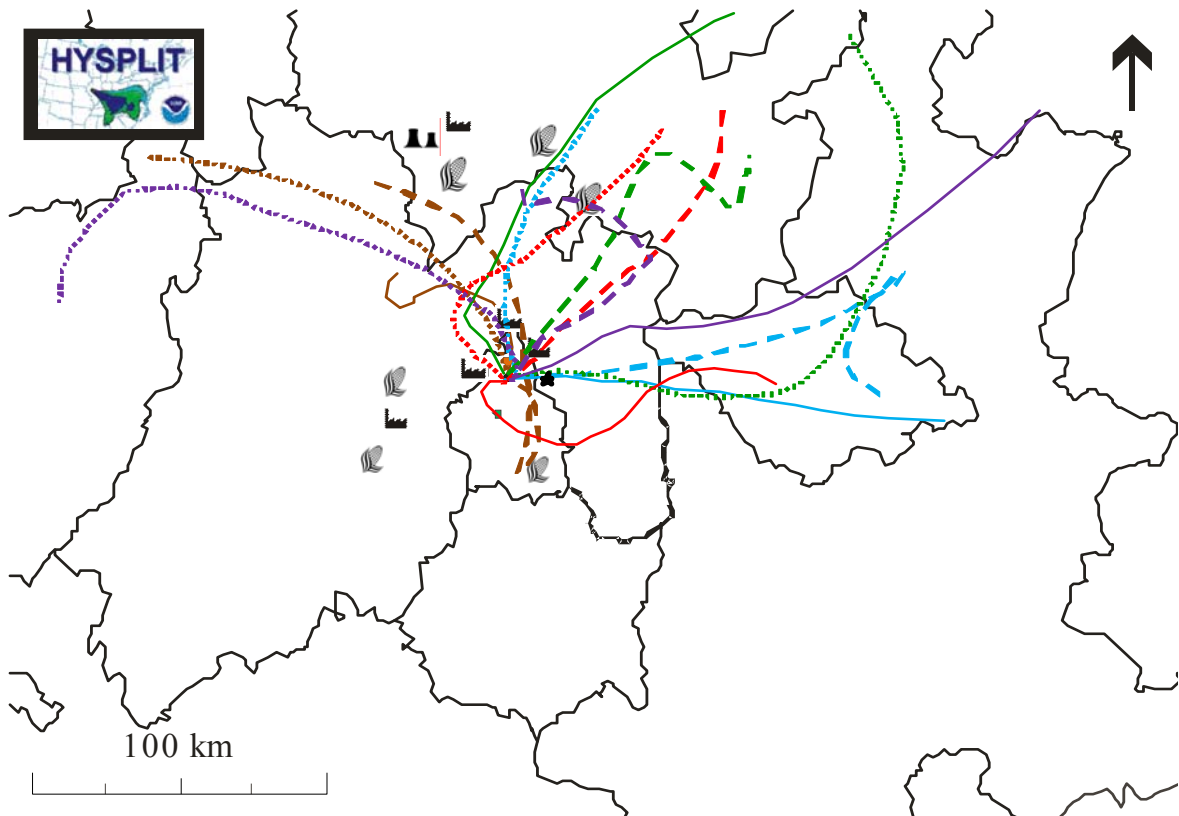


Fig. 11. Concentration ratios relative to Si for PM₁₀ fugitive dust sources determined by Vega et al. (2001) and for the “soil” factors obtained with PMF

particles. Nevertheless, it must be recalled that the transit of a trajectory above or from a specific area may be a hint of a possible source contributing to particulate matter at the sampled site, but it is not enough to assure the origin. Although HYSPLIT has been applied by other authors (Báez *et al.*, 2007), no specific association between the back-trajectories and the so-called crustal elements was given. In this work, it was found that most of the “soil” and “sulfate” events came from the northeast and east, with a few directions from the west. In this regard, Fig. 12 shows examples of the results associated to “soil” and “sulfate” episodes. The dates are January 7, February 12, and May 4 for “soil”; February 15 and May 10 for “sulfate”. In the first case, there is an episode around that date registered in the three sites; the application of HYSPLIT describes back-trajectories coming from the north of the sampling sites, some of them also passing above the dry Texcoco Lake, in accordance with what was expected from other authors’ results (Moya *et al.*, 2003). The strong episode observed for “soil 2” in the South is associated with back-trajectories also from east and north. The next episode shown (May 4) is associated with back-trajectories definitely crossing the dry lake. Results achieved with HYSPLIT are in complete agreement also with μ PIXE findings, with important number of particles with elements Si, K, Ca, Ti, and Fe. The back-trajectory for February 15, connected to an episode in “sulfate” factors for the three sites, corresponds to an east origin; this path crosses the heavily polluted and

industrialized area of Xalostoc. The SO₂ data from SIMAT (2009), collected in the Xalostoc automatic station in the days around this date are displayed in Fig. 13, together with the concentrations predicted for the “sulfate” factors in the three sites. There are maxima in the values for all the variables, strongly suggesting there is a correlation between SO₂ and the presence of secondary aerosols, produced when “soil” particles cross areas with high contents of this gas. A completely similar compartment is found for the data in May 10, but in this case the back-trajectories come from the western area of the MAMC. There are no available SO₂ data for stations along the back-trajectories, but is noted that they come over the Naucalpan industrial which is also expected to have high SO₂ contents. This result favors “local” chemical reactions of the aerosols with SO₂ rather than long-range transport. The remaining episodes for “soil” and “sulfate” are in concordance with the examples shown, having “soil” sources from the north and east of the sampling sites, and “sulfate” crossing industrial areas (northeast, northwest and north of the MAMC). Only in a few cases (like the episode in April 4), the provenance of particulate matter from the Toluca Valley agrees with the observations by Johnson *et al.* (2006). Furthermore, it is highly probable that the Tula refinery and thermoelectric power plant are reacting with the “soil” particles, giving origin to the “soil 1” in the Center, “soil” in the North, and “soil 1” in the South. These factors show elevated S contents.



— January 7 Soil — February 12 Soil — May 4 Soil — February 15 Sulfate — May 10 Sulfate

Fig. 12. Back-trajectories predicted by HYSPLIT for Soil and Sulfate episodes found at different dates. The continuous, dotted and dashed curves represent back-trajectories starting 24 h, 18 h and 12 h before the ending of the sample collection, respectively. The symbols represent: industrial areas; agricultural areas; * Texcoco Lake; Tula thermoelectric power plant. Trajectories shown correspond to a 500 m above ground level height

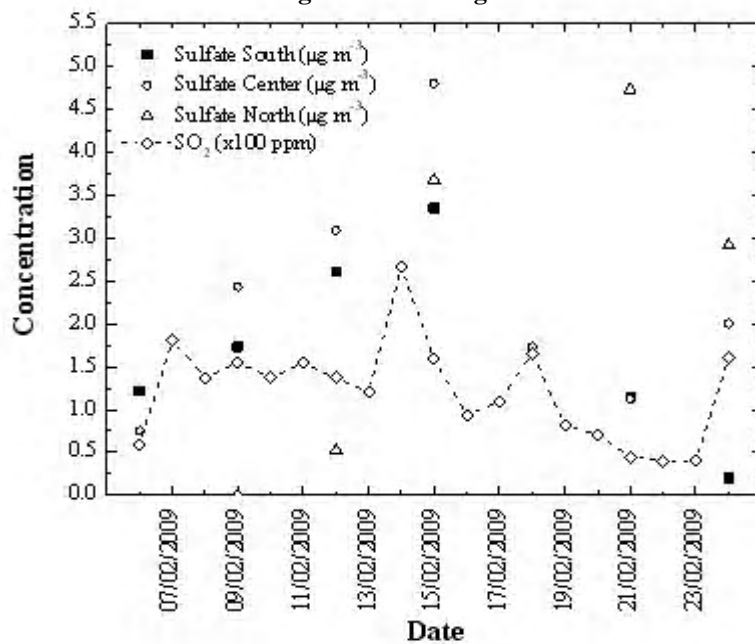


Fig.13. Concentrations of SO_2 measured by SIMAT (2009), collected in the Xalostoc automatic station in the days around February 12, as compared with the concentrations predicted for the Sulfate factors in the three sites

With regard to the behavior of “biomass burning” particles, it is helpful to make use of the open access resource known as Web Fire Mapper (<http://maps.geog.umd.edu/firms/>), which is a part of MODIS41,45 (moderate-resolution imaging spectroradiometer) (Justice *et al.*, 2002). This is carried out in conjunction with the HYSPLIT back-trajectories. There are several episodes for the “biomass burning” factors in the three sites, namely, January 7 in the North, January 19 in the North and Center, and May 28 in the South site. Fig. 14 displays probable fire spots obtained around those dates, together with the simulations by HYSPLIT. In all the cases, it was observed that those fires were only present during the episodes. For January 7, it is shown how two fire sites are located very near to the North sampling site; therefore, it is not surprising to see this sudden growth in the “biomass burning”

factor and not in the other two sites. For February 19, the back-trajectories come from the north, east and south of the MAMC, right above several observed fire spots. Finally, the episode in the South during May 28 is related to numerous fires in the west of the MAMC, with back-trajectories coming precisely from that area. As a whole, the results for biomass burning are completely coherent, including the mappings obtained with μ PIXE (Fig. 9), where particles with the Cl-K combination are found.

Although it is highly desirable to apply CMB methods to the present study, it was not possible, because the sources identified with PMF do not correspond exactly to any of the already characterized fugitive dust sources (Vega *et al.*, 2001). Thus, as mentioned by Shivastava *et al.* (2007): “CMB requires *a priori* knowledge of source profiles that represent

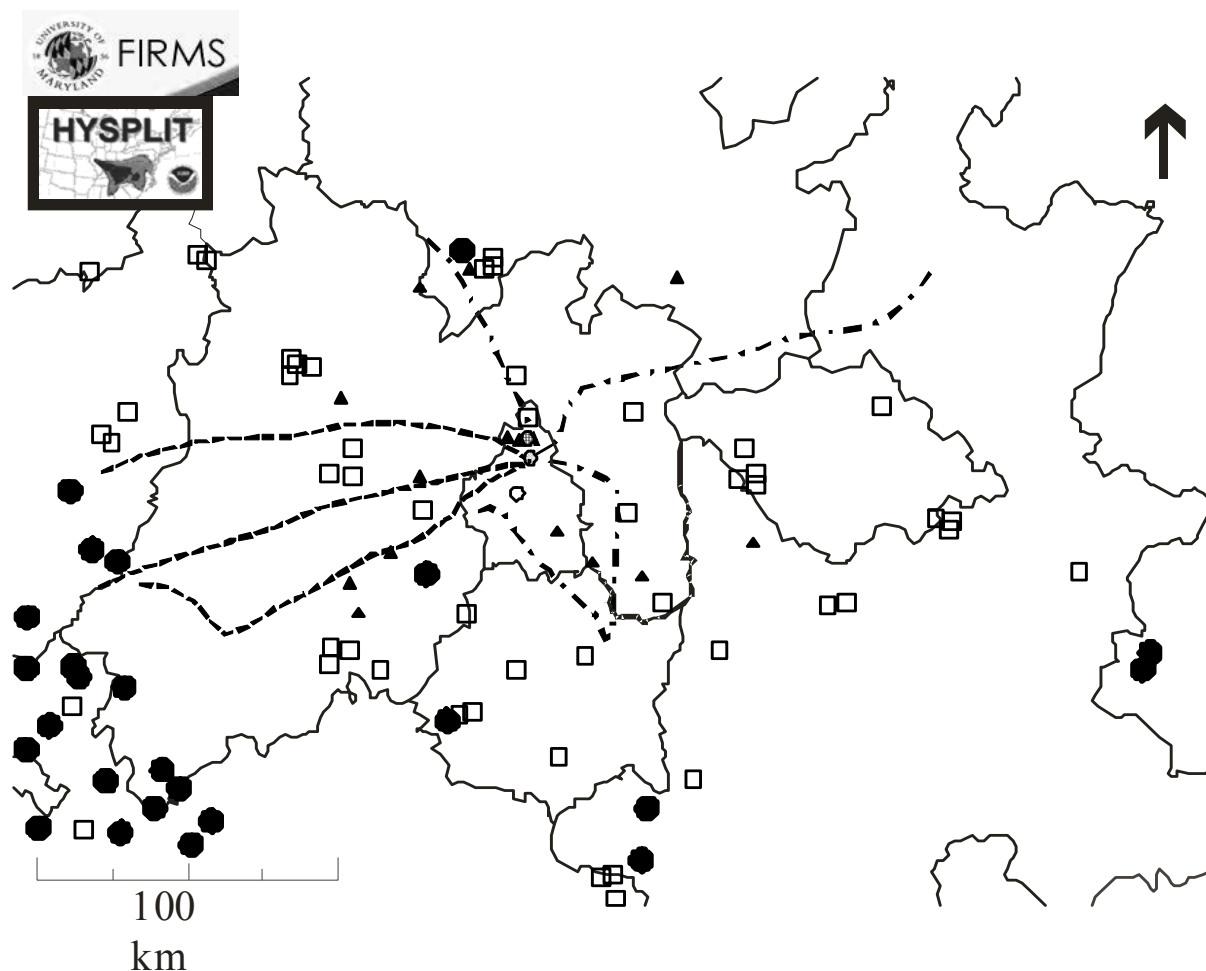


Fig. 14. Fire spots determined by the Web Fire Mapper during January 7 (black triangles), January 19 (empty squares), May 28 (black circles), and back-trajectories predicted by HYSPLIT for January 19 (dash-dotted curve), and May 28 (dashed curve). The dates correspond to episodes in the Biomass burning factors

the aggregate emissions from all sources in a given source class. Selecting source profiles is complicated because most profiles are based on a single or a small number of source tests and multiple profiles have been developed for important source classes such as motor vehicles. This creates substantial uncertainty because CMB results can depend strongly on which profiles are included in the model". This task is even more difficult here because many of the soil-based particles seem to be strongly influenced by chemical reactions with, for instance, SO₂, a fact observed simultaneously with μ PIXE, through the PMF model, the SO₂ measured concentrations, and the HYSPLIT simulations. The present work, therefore, should encourage a wider characterization of sources of soil-derived airborne particulate matter.

CONCLUSION

The results presented in this work emphasize the need of using different tools to obtain more reliable results in the study of atmospheric aerosols. In this case, the main goal was to identify the possible provenance of certain types of aerosols, X-ray spectrometric methods were good enough to attain this objective. In spite of not being able to provide information about other very important compounds (nitrates, elemental and organic carbon, oxygen), the determination of contents of certain elements considered as source "markers" allowed the identification of their possible origin. Regarding the development of receptor models through PMF, it is necessary to stress the fact that they describe very well the general behavior of the measured gravimetric mass, giving reasonable identification of polluting sources. It is not required to have information on the trace elements (such as Cr, Ni, Cu, Se, Pb), but only on "major" elements, to find the geological, biomass burning, or secondary aerosols (sulfate) potential emitters. A more extensive characterization of possible sources of geological material must be carried out in the future. Although the work by Vega et al. (2001) is a useful guide for the partial understanding of the present results, the composition of those sources is highly affected by chemical processes with other compounds present in the atmosphere during transport to the sampling sites. The application of μ PIXE allowed the confirmation of the existence of secondary aerosols, namely, soil-derived particles subjected to chemical reactions with atmospheric SO₂ or other S-related chemically active ions, as well as of biomass burning particles. Whether there is a long-range transport or a short one producing secondary aerosols may require further investigations, but the present

results coincide with a "local" phenomenon. The concurrence of episodes in Sulfate factors and SO₂ concentrations in industrial zones support this assertion. The use of HYSPLIT and the MODIS database to explain the episodes helped to support the results published by other authors, namely, that both the Texcoco Lake and to a lesser extent the Toluca Valley contribute to soil-derived aerosols, while fire spots located around the MAMC produce high concentrations of particulate matter in the urban area. Finally, it is suggested to use other models with a better spatial resolution to determine back-trajectories, to find out the possible existence of short-range sources.

ACKNOWLEDGEMENTS

The support of CONACYT and *Posgrado de Ciencias de la Tierra*, UNAM, is acknowledged by VAB, for scholarships. The authors thank Prof. P. Paatero for kindly providing PMF computer programs, as well as J.I. Cruz, M. Cuautle, F. Mercado, and M.A. Veytia for technical support. The authors gratefully acknowledge the NOAA Air Resources Laboratory (ARL) for the provision of the HYSPLIT transport and dispersion model and/or READY website (<http://www.arl.noaa.gov/ready.php>) used in this publication, as well as the support of the *Programa de Estaciones Meteorológicas del Bachillerato Universitario, Centro de Ciencias de la Atmósfera*, UNAM, for allowing access to meteorological data.

REFERENCES

- Báez, P. A., García, M. R., Torres, B. M. del C., Padilla, H. G., Belmont, R. D., Amador, O. M. and Villalobos-Pietrini, R. (2007). Origin of trace elements and inorganic ions in PM₁₀ aerosols to the South of Mexico City. *Atmos. Res.*, **85**, 52–63.
- Barfoot, K. M., Vargas-Aburto, C., MacArthur, J. D., Jáidar, A. and García-Santibáñez, F. (1984). Multi-elemental measurements of air particulate pollution at a site in Mexico City. *Atmos. Environ.*, **18**, 467–471.
- Chiou, P., Tang, W., Lin, C. J., Chu, H. W. and Ho, T. C. (2009). Comparison of Atmospheric Aerosols between Two Sites over Golden Triangle of Texas. *Int. J. Environ. Res.*, **3**, 253-270.
- Cohen, D. D., Crawford, J., Stelcer, E. and Bac, V. T. (2010). Characterisation and source apportionment of fine particulate sources at Hanoi from 2001 to 2008. *Atmos. Environ.*, **44**, 320-328.
- De Foy, B., Varela, J. R., Molina, L. T. and Molina, M. J. (2006). Rapid Ventilation of the Mexico City Basin and Regional Fate of the Urban Plume. *Atmos. Chem. Phys.*, **6**, 2321–2335.

- Draxler, R. R. and Rolph, G. D. (2010). HYSPLIT Hybrid Single-Particle Lagrangian Integrated Trajectory) Model access via NOAA ARL READY Website (<http://ready.arl.noaa.gov/HYSPLIT.php>). (NOAA Air Resources Laboratory, Silver Spring, MD).
- EPA, (2010). Environmental Protection Agency, EPA Positive Matrix Factorization (PMF) 3.0 Model. Retrieved April 14, 2011 from <http://www.epa.gov/heasd/products/pmf/pmf.html>.
- Espinosa, A. A., Miranda, J. and Pineda, J. C. (2010). Evaluation of uncertainty in correlated quantities: application to elemental analysis of atmospheric aerosols. *Rev. Mex. Fis. E* 56, 134-140. Retrieved April 14, 2011 from (http://rmf.fciencias.unam.mx/pdf/rmf-e/56/1/56_1_0134.pdf; and http://www.fisica.unam.mx/pixe2007/Downloads/Proceedings/PDF_Files/PIXE2007-PI-26.pdf)
- Hopke, P. K. (1991). Receptor modeling for air quality management. Ed. (Elsevier, Amsterdam).
- IAEA, (1997). Manual for QXAS, International Atomic Energy Agency, Vienna.
- Jeong, J.-I. and Park, S.-U. (2008). Interaction of gaseous pollutants with aerosols in Asia during March 2002. *Sci. Tot. Environ.*, **392**, 262–276.
- Johnson, K. S., de Foy, B., Zuberi, B., Molina, L. T., Molina, M. J., Xie, Y., Laskin, A. and Shutthanandan, V. (2006). Aerosol composition and source apportionment in the Mexico City Metropolitan Area with PIXE/PESA/STIM and multivariate analysis, *Atmos. Chem. Phys.*, **6**, 4591–4600.
- Justice, C. O., Giglio, L., Korontzy, S. and Owen, J. (2002). The MODIS fire products. *Remote Sensing Environ.*, **83**, 244-262.
- Maxwell, J. A., Teesdale, W. J. and Campbell, J. L. (1995) *Nucl. Instrum. Methods B*, **95**, 407-421.
- Miranda, J., López-Suárez, A., Paredes-Gutiérrez, R., González, S., De Lucio, O. G., Andrade, E., Morales, J. R. and Avila-Sobarzo, M. J. (1998). A study of atmospheric aerosols from five sites in Mexico city using PIXE. *Nucl. Instrum. Methods B*, **136-138**, 970-974.
- Miranda, J., Barrera, V. A., Espinosa, A. A., Galindo, O. S., Núñez-Orosco, A., Montesinos, R. C., Leal-Castro, A., and Meinguer, J. (2004). PIXE analysis of atmospheric aerosols from three sites in Mexico City. *Nucl. Instrum. Methods B*, **219-220**, 157-160.
- Miranda, J., Barrera, V. A., Espinosa, A. A., Galindo, O. S. and Meinguer, J. (2005). PIXE analysis of atmospheric aerosols in Mexico City. *X-Ray Spectrom.*, **34**, 315-319.
- Miranda, P. A., Chesta, M. A., Cancino, S. A., Morales, J. R., Dinator, M. I., Wachter, J. A. and Tenreiro, C. (2006). Recent IBA setup improvements in Chile. *Nucl. Instrum. Methods B*, **248**, 150-154.
- Molina, L. T., Madronich, S., Gaffney, J. S., Apel, E., De Foy, B., Fast, J., Ferrare, R., Herndon, S., Jimenez, J. L., Lamb, B., Osornio-Vargas, A. R., Russell, P., Schauer, J. J., Stevens, P. S. and Zavala, M. (2010). An overview of the MILAGRO 2006 campaign: Mexico City emissions and their transport and transformation. *Atmos. Chem. Phys.*, **10**, 8697-8760.
- Montero Lorenzo, J. M., Garcia-Centeno, M. C. and Fernandez-Aviles, G. (2011). A Threshold Autoregressive Asymmetric Stochastic Volatility Strategy to Alert of Violations of the Air Quality Standards. *Int. J. Environ. Res.*, **5** (1), 23-32.
- Moya, M., Castro, T., Zepeda, M. and Báez, A. (2003). Characterization of size-differentiated inorganic composition of aerosols in Mexico City. *Atmos. Environ.*, **37**, 3581–3591.
- Navarrete, M., Gálvez, L., Tzontlimatzin, E. and Aguilar, C. (1974). Determination of particulate air pollutants in Mexico City using activation analysis. *Radiochem. Radioanal. Lett.*, **19** (3), 163-170.
- Nejadkoorki, F. and Baroutian, S. (2012). Forecasting Extreme PM10 Concentrations Using Artificial Neural Networks, *Int. J. Environ. Res.*, **6** (1), 277-284.
- Paatero, P. and Tapper, U. (1994). Positive Matrix Factorization – a Nonnegative Factor Model with Optimal Utilization of Error-Estimates of Data Values. *Environmetrics*, **5**, 111–126.
- Querol, X., Pey, J., Minguillón, M. C., Pérez, N., Alastuey, A., Viana, M., Moreno, T., Bernabé, R. M., Blanco, S., Cárdenas, B., Vega, E., Sosa, G., Escalona, S., Ruiz, H. and Artiñano, B. (2008). PM Speciation and Sources in Mexico during the MILAGRO-2006 Campaign. *Atmos. Chem. Phys.*, **8**, 111–128.
- Rolph, G. D. (2010). Real-time Environmental Applications and Display sYstem (READY) Website (<http://ready.arl.noaa.gov>). (NOAA Air Resources Laboratory, Silver Spring, MD).
- Shrivastava, M. K., Subramanian, R., Rogge, W. F. and Robinson, A. L. (2007). Sources of organic aerosol: Positive matrix factorization of molecular marker data and comparison of results from different source apportionment models. *Atmos. Environ.* 41, 9353-9369.
- SIMAT, (2009). Simat Technical Resources, Retrieved April 14, 2011 from <http://www.sma.df.gob.mx/simat2/informaciontecnica/index.php>.
- Speciate, (2009). Speciate 4.2 Speciation Database Development Documentation (Environmental Protection Agency, Washington, DC).
- Statsoft (1993). *Statistica/W*, Statsoft, Tulsa, OK, USA.
- Vega, E., Mugica, V., Reyes, E., Sánchez, G., Chow, J. C. and Watson, J. G. (2001). Chemical composition of fugitive

dust emitters in Mexico City. *Atmos. Environ.*, **35**, 4033-4039.

Vega, E., Eidels, S., Ruiz, H., López-Veneroni, D., Sosa, G., González, E., Gasca, J., Mora, V., Reyes, E., Sánchez-Reyna, G., Villaseñor, R., Chow, J. C., Watson, J. G. Edgerton, S. A. (2010). Particulate Air Pollution in Mexico City: A Detailed View. *Aerosol and Air Quality Res.*, **10**, 193-211.

Voss, P. B., Zaveri, R. A., Flocke, F. M., Mao, H., Hartley, T. P., DeAmicis, P., Deonandan, I., Contreras-Jiménez, G., Martínez-Antonio, O., Figueroa Estrada, M., Greenberg, D., Campos, T. L., Weinheimer, A. J., Knapp, D. J., Montzka, D. D., Crouse, J. D., Wennberg, P. O., Apel, E., Madronich, S. and de Foy, B. (2010). Long-range pollution transport during the MILAGRO-2006 campaign: a case study of a major Mexico City outflow event using free-floating altitude-controlled balloons. *Atmos. Chem. Phys.*, **10**, 7137-7159.

Zou, B., Zhan, F. B., Zeng, Y., Yorke, Ch. and Liu, X. (2011). Performance of Kriging and EWPM for Relative Air Pollution Exposure Risk Assessment. *Int. J. Environ. Res.*, **5** (3), 769-778.